Semi-Automated Repair Verification of Aerial Images

Eric Poortinga[1], Thomas Scheruebl[2], Rigo Richter[2]
[1]Carl Zeiss SMT Inc. (USA)
[2]Carl Zeiss SMS GmbH (Germany)
One Corporation Way, Peabody, MA 01960
Phone: +1-646-725-3191 Fax: +1-512-246-7301 Email: poortinga@smt.zeiss.com

ABSTRACT

Using aerial image metrology to qualify repairs of defects on photomasks is an industry standard. Aerial image metrology provides reasonable matching of lithographic imaging performance without the need for wafer prints. Utilization of this capability by photomask manufacturers has risen due to the increased complexity of layouts incorporating RET and phase shift technologies. Tighter specifications by end-users have pushed aerial image metrology activities to now include CD performance results in addition to the traditional intensity performance results.

Discussed is the computer implemented semi-automated analysis of aerial images for repair verification activities. Newly designed user interfaces and algorithms could guide users through predefined analysis routines as to minimize errors. There are two main routines discussed here, one allowing multiple reference sites along with a test/defect site on a single image of repeating features. The second routine compares a test/defect measurement image with a reference measurement image.

This paper highlights new functionality desirable for aerial image analysis as well as describes possible ways of its realization. Using structured analysis processes and innovative analysis tools could lead to a highly efficient and more reliable result reporting of repair verification metrology.

Keywords: photomask, repair, AIMS, CD control, aerial image

1. INTRODUCTION

The aerial image measurement system (AIMS™) developed by Carl Zeiss more than a decade ago has become the industry standard tool for the verification of repairs made to photomasks. This was born out of the importance of defect free photomasks in the lithographic process of semiconductor manufacturing. Nearly all repair techniques leave the defective area of the photomask in less than perfect or ideal condition. Under high magnification, such as when using scanning electron microscopy (SEM), it is evident that a defect has been fixed through the removal or adding of material. A methodology to verify that the defect was fixed and that the repair process itself did not create additional defects was needed. Through close collaboration with International Business Machines in the 1990's, a method of using an emulated aerial image, based on the same lithographic parameters as used in the wafer fab, for repair verification was developed.[1]

Because the aerial image is unperturbed by factors other than the photomask and optical conditions, it makes an ideal criteria to base defect printability and repair verification measurements. The AIMS™ methodology allows similar illumination settings, that are user adjustable, to match the conditions used at the wafer fab. The wavelength of light is the same (248nm or 193nm depending on technology), coherence type is similar, and the incidence to the photomask is the same. On the imaging side, the numerical aperture (NA) is also adjustable to match that of the wafer scanner. The main difference is that the photomask pattern is projected on to a CCD instead of a photoresist-coated wafer. This difference requires AIMS™ tools to post-magnify the projected image in order to accommodate resolution requirements with respect to CCD pixel size. On the MSM and AIMS™ fab platforms, this technique provides suitable matching to wafer scanner results. When using high NA, industry consensus is >0.8NA, the polarized components of the diffracted light that form the projected image must be taken into account to ensure correct contrast. With the introduction of the

Photomask and Next-Generation Lithography Mask Technology XVI, edited by Kunihiro Hosono
Proc. of SPIE Vol. 7379, 73792D · © 2009 SPIE · CCC code: 0277-786X/09/$18 · doi: 10.1117/12.824327

AIMS™45-193i system in 2006 a solution was developed to compensate for the inability of the magnified image to inherently capture so-called vector effects.[2]

As improvements to the hardware of the AIMS™ platform have kept pace with technological improvements to wafer scanners, so have software applications progressed. The MSM platform was more or less a research tool with manual controls and rudimentary operating software. The analysis software provided very basic and manually driven image analysis that reported simple intensity and CD through-focus data. The AIMS™fab platform moved aerial image measurements into the manufacturing realm. The operating software allowed automated acquisition of images and the analysis software provided dynamic options for interpreting the results.

The AIMS™45-193i takes those improvements to the next level by providing aerial image measurement capability to high volume photomask manufacturers[3,4]. Options such as global alignment using pattern-recognition, improved auto-focus algorithms, batching of recipes, and SECS\GEM integration have increased the throughput and utilization rates. The timing of these improvements corresponds to an industry need to qualify more photomasks with an increasing number of sites using aerial image measurements. This is due to advances in reticle enhancement techniques (RET) and the use of phase shift materials[5] that have led to highly complex layouts on the photomask. Furthermore, recent approaches like Computational Lithography and Source Mask Optimization lead to highly complex patterns on the reticle[6]. The ability to easily identify critical features has been lost. Aerial image measurements are the most effective method to predict the final printed image quality on advanced photomasks of today.

Larger volumes of acquired aerial images leads to a larger amount of time spent analyzing those images. This coupled with an improvement in defect repair technologies, which has made it harder to identify the previous position of a defect, has created the necessity to discuss possible improvements of the AIMS™ analysis capability.

2. METHODOLOGY

Users provided feedback that the standard process flow for analyzing a typical defect repair was too manual in nature. This situation gave rise to user errors and an inconsistent process between users which generated additional cost. The amount of time analysis took was also an issue because it leads to an extended period before the photomask could be moved onto the next manufacturing step. More advanced analysis techniques became mandatory to engineers that want to garner more information about a specific repair or defect.

From these requirements, a framework was created that serves as the basis of possible functions of new software applications. The application would need to follow a structured analysis process as to limit user errors. It should also be integrated into the operational software so time is not wasted moving between interfaces when analysis on the AIMS™ tool is required. Also, new and innovated analysis tools should be developed that allow thorough result reporting on advanced photomasks. The way results are reported should also be customizable by the user to fit manufacturing process needs. All of these tasks should be automated as much as possible to further reduce user errors and increase throughput and reliability of the data.

The architecture of a possible application discussed here should be divided into two main components: Multi-Slice Analysis (MSA) and Image Compare (IC).

The MSA component is intended for aerial images that consist of a repeating pattern within the acquisition field **(see Figure-1)**. When this component is initialized, the user has the ability to define measurement slices over multiple reference features. The user also defines a measurement slice over a feature in the area that the defect resides or the area fixed by repair. The setup of the slices is automatically recorded in a table within the plug-in interface. The table lists the position within the image, the length, the width, and angle of the measurement slice. There is also an option to automatically copy the length, width, and angle to remaining slices.

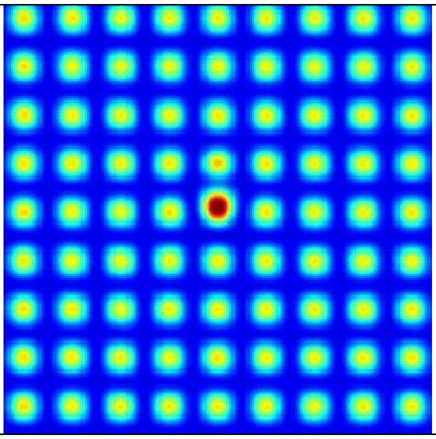

Figure-1: Repeating array of identical contact-holes, suitable for MSA analysis

After the measurement slices are defined, the user switches the table type from the setup style to an analysis style. The user then defines a common reference intensity threshold or an associated target reference CD. If a target reference CD is used, the software automatically calculates the intensity threshold that correlates to that CD. The result values from each measurement slice are updated in real-time. The setup of the analysis table style is user-configurable and can output a number of values including CD, Intensity, Normalized Image Log Slope (NILS), and Depth of Focus (DOF) for all the measurement slices. Analytics can also be defined to automatically calculate the absolute delta or percent difference between the test slice and an average of the reference slices.

The other component is the Image Compare component. The IC process is intended for aerial images that are in defect/reference or repair/reference pairs **(see Figure-2)**. Typically, this is possible with multiple-die photomask layouts where each die is identical. The IC interface steps the user through the process of defining an intensity threshold using the reference image (with the ability to use a target CD instead), correlates the images so that they are perfectly overlaid, and provides various option to identify out-of-spec areas of the defect or repair image.

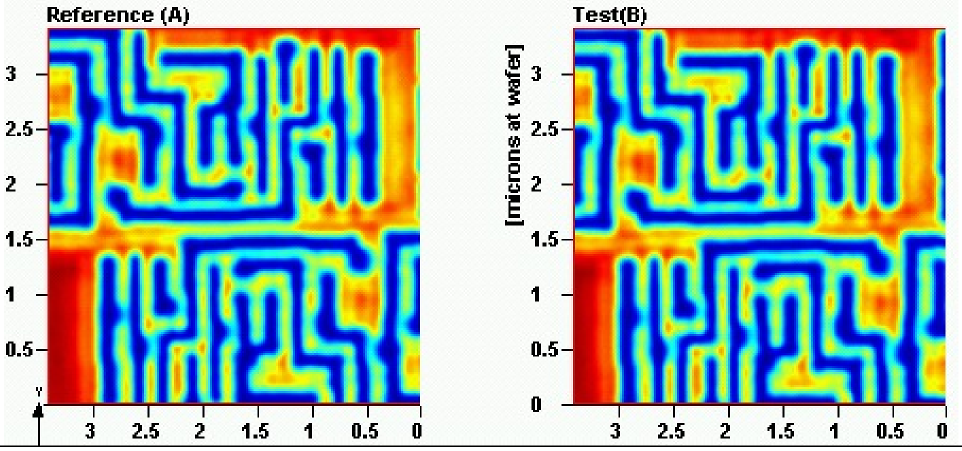

Figure-2: Test and Reference image pair, suitable for Image Compare analysis

The IC interface introduces new techniques to correlate and overlay the image pairs. Users have the option of selecting between an Intensity-based and a Contour-based correlation algorithm. The Intensity-based algorithm adjusts the offset between the two images so that the number of matching pixels using intensity values is maximized. The Contour-based algorithm uses the reference threshold found in the preceding step to generate the 2-dimensional contours of each image, and then adjusts the offset between them to maximize the amount of overlap between the contour lines. Also discussed is the ability to define a correlation region of interest. Only the section of image inside the region of interest is used to determine the correlation offset. This allows the user to exclude the defect area which would lower the accuracy of the correlation algorithm. An error value for the correlation result is displayed to the user to assist in determining the effectiveness of the user's correlation setup.

Four options are available to the user to determine out-of-spec areas of the defect or repair image inside the IC interface. The first option is the ability to display a plot of the overlaid contours with edge differences highlighted **(see Figure-3a)**. If the defect or repair image contour is bigger then the reference image contour, the area between the contour edges is highlighted gray. If the difference is defect or repair image contour is smaller, the difference is highlighted red. To assist the user in finding only differences that are significant, a tolerance value is available. The user can input a tolerance that turns-off the highlighting if the difference between the contour edges is below the defined tolerance.

Another option is the ability to display a plot of the intensity differences between the image pair **(see Figure-3b)**. The reference image is subtracted from the defect/repair image and the result is displayed. If the user's result criterion includes intensity differences, then this would allow the user to easily find those types of errors in the images.

If the user is interested in finding deviations in the percent difference between the defect/repair CD compared to the reference CD of a feature, the Defect Highlighting option provides this data **(see Figure-3c)**. The CD percent difference is calculated at every position in the image contour. The user chooses which measurement direction and feature type, line or space, should be evaluated. The software automatically highlights all features that do not meet a user defined specification limit.

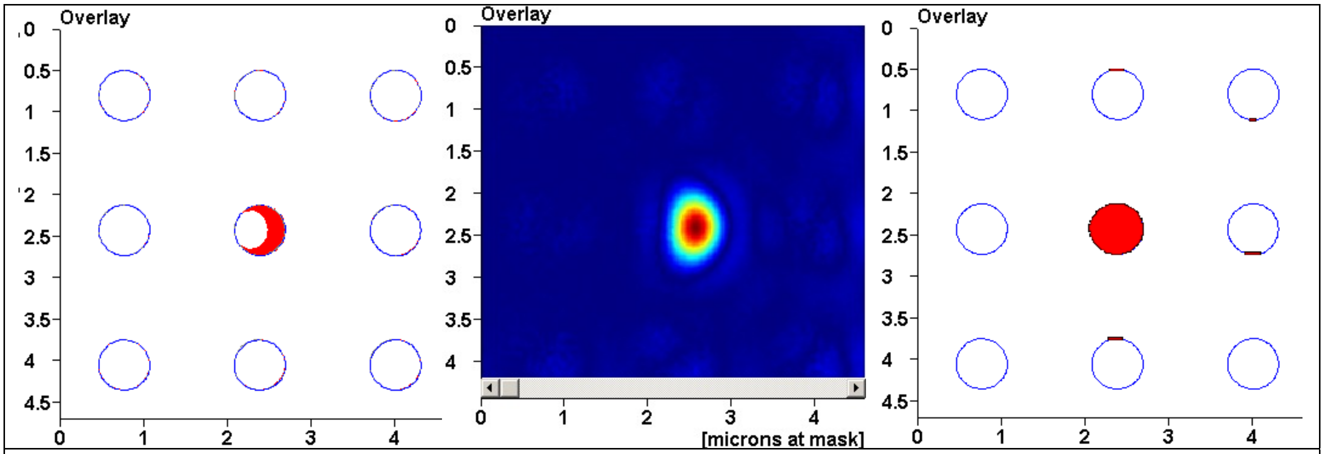

Figures-3a-c: left: contour edge difference, center: intensity difference, right: highlighting %CD difference

With these analysis options, the user is still required to manually draw measurement slices over desired highlighted regions of the plots. The slices can be added to the analysis result table, storing the slice positions into memory for easy switching between slices.

The fourth and final analysis option is a fully automatic function that defines a measurement slice over the feature with the maximum contour edge difference. The user only is required to press a single button inside the interface and the measurement slice is automatically defined after a short calculation is executed. This automatic slice can also be added to the analysis result table.

For each measurement slice, the Intensity Profile plot shows not only the intensity data for each image overlaid, but also shows the absolute difference and calculated percent difference. The Linewidth versus Threshold plot shows the through-focus CD values for each image at the pre-defined reference threshold and a chart of the through-focus absolute CD difference and percent difference. All of these values can be exported by the user in a text file.

3. EXAMPLES

3.1. MSA Contact-hole example

The first example is using a contact-hole array with an undersized contact-hole. This type of pattern lends itself to be analyzed using the MSA component. After opening the AIMS™ image and the MSA component is initialized from a toolbar icon, the user is presented with a four-pane window. The upper-left pane displays the image plot, the upper-right pane displays the Intensity Profile plot, the lower-left pane displays the Linewidth vs. Threshold plot, and the lower-right pane is the MSA working window. Initially the measurement setup styled table is displayed. The user can then draw a measurement slice over the test region of the image, in this case the undersized contact-hole. This example will use horizontal slices, but the user is free to choose any orientation. The first reference slice row in the table is selected and then the corresponding slice can be drawn in the image plot. Additional reference slices can be added by repeating this process. In this example, four reference slices are added, one to the left, to the top, to the right, and to the bottom of the test region.

The user then switches the table of the MSA working window to the analysis styled table **(see Figure-4)**. Using the table as a reference, the slice positions can be moved to the center of the contact-holes by looking for the maximum intensity value for that slice. Once this is completed, a target CD value can be entered into the entry box, and the software automatically calculates the threshold. In this example, a target CD value of 0.600um was entered and a threshold of 0.352 was found. The analysis table shows an absolute CD difference of -0.204um that corresponds to a -34.0% difference.

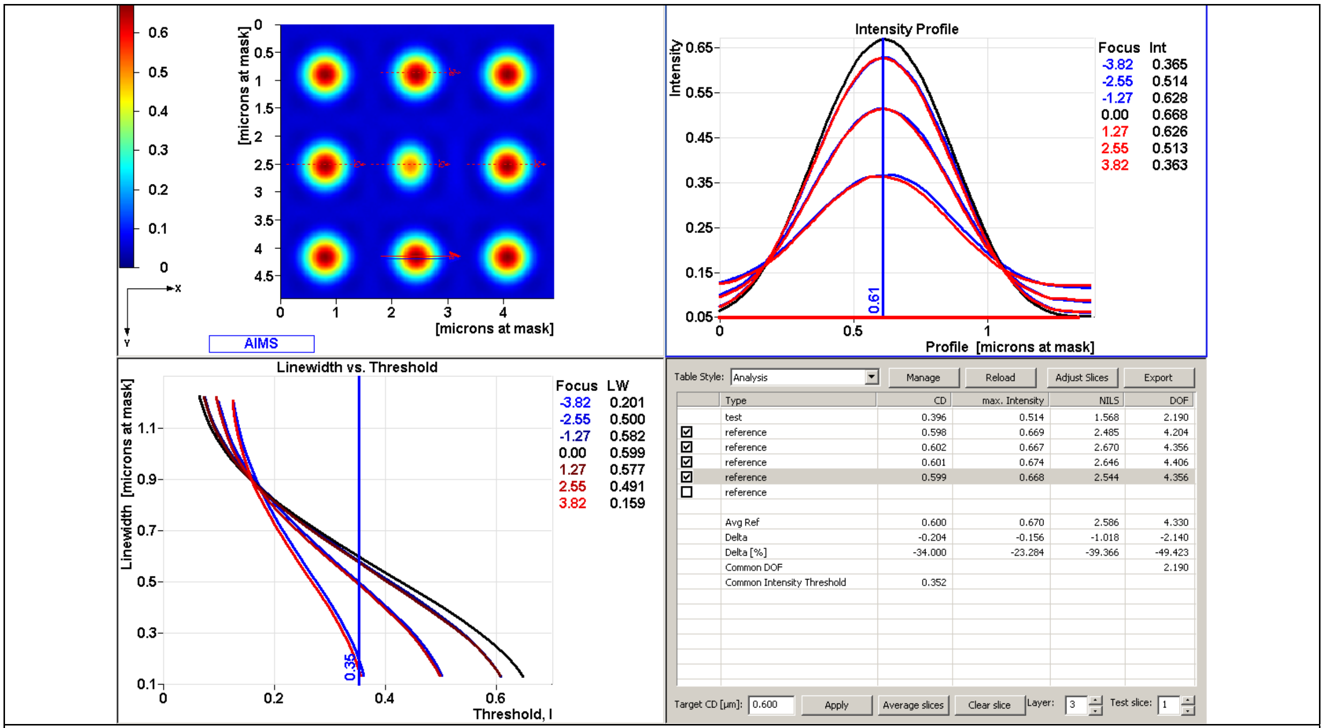

Table Style: Analysis

	Type	CD	max. Intensity	NILS	DOF
	test	0.396	0.514	1.568	2.190
☑	reference	0.598	0.669	2.485	4.204
☑	reference	0.602	0.667	2.670	4.356
☑	reference	0.601	0.674	2.646	4.406
☑	reference	0.599	0.668	2.544	4.356
☐	reference				
	Avg Ref	0.600	0.670	2.586	4.330
	Delta	-0.204	-0.156	-1.018	-2.140
	Delta [%]	-34.000	-23.284	-39.366	-49.423
	Common DOF				2.190
	Common Intensity Threshold	0.352			

Target CD [µm]: 0.600
Layer: 3
Test slice: 1

Figure-4: Multi-Slice Analysis result table of undersized contact-hole

3.2. IC Contact-hole example

The same contact-hole array can be analyzed using the Image Compare functionality if a reference image should also be available. There are two ways to initiate the IC interface; the easiest by selecting both the defect and reference image simultaneously in the MSM Browser window, right clicking the mouse on the screen, and selecting "Compare both selected images" from the option list that appears. When references are acquired in the AIMS™ measurement wizard, the images are tagged as being a reference in the save file, allowing the IC interface to distinguish the pair automatically.

The user is presented with a four-pane window. Different to the MSA component, the upper-left pane is now the reference image plot. The lower-right pane is a table to define reference measurement slices. A slice over a reference feature is drawn in the image plot, then the target CD is entered or a known intensity threshold can be input, after which this slice is added to the table. At least one reference measurement must be made, and if multiple references are used, the average intensity threshold is calculation. This value is used throughout the rest of the analysis. The user can then press the "Next" button.

The window changes by showing a new interface used to setup the correlation of the image pair. Both the reference image and defect image is shown at the top of the window and the user options are listed at the bottom. Once the correlation is setup, the "Execute" button starts the calculation to determine the image offsets, which are then applied. Pressing the "Next" button again changes the window one final time.

A four-pane analysis window is displayed to the user as shown in **Figure-5**. The upper-left pane content is determined by the option the user selects in the lower-right pane. Choosing the Contour-Diff view type highlights the under-sized contact-hole quite prominently. Pressing the "Auto Slice" button in the lower-right pane automatically draws a slice across the largest difference between the reference and defect contour edges. Pressing the "Add Slice" button saves this slice position to the result table. An intensity difference of nearly -90% and a CD difference of over 33% is found. The results could then be exported to finish a basic analysis process. Not only does this function help identify out-of-spec features, but this analysis would be nearly impossible to perform manually with the traditional AIMS™ software.

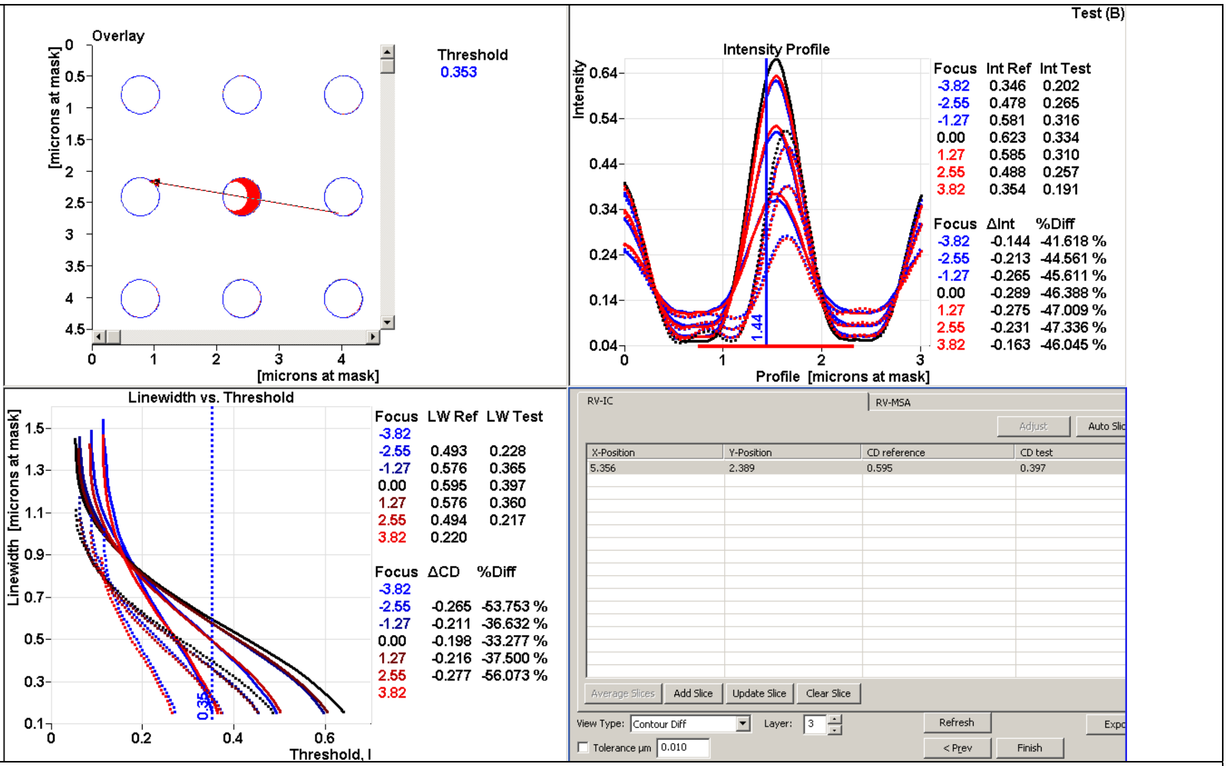

Focus	Int Ref	Int Test
-3.82	0.346	0.202
-2.55	0.478	0.265
-1.27	0.581	0.316
0.00	0.623	0.334
1.27	0.585	0.310
2.55	0.488	0.257
3.82	0.354	0.191

Focus	ΔInt	%Diff
-3.82	-0.144	-41.618 %
-2.55	-0.213	-44.561 %
-1.27	-0.265	-45.611 %
0.00	-0.289	-46.388 %
1.27	-0.275	-47.009 %
2.55	-0.231	-47.336 %
3.82	-0.163	-46.045 %

Focus	LW Ref	LW Test
-3.82		
-2.55	0.493	0.228
-1.27	0.576	0.365
0.00	0.595	0.397
1.27	0.576	0.360
2.55	0.494	0.217
3.82	0.220	

Focus	ΔCD	%Diff
-3.82		
-2.55	-0.265	-53.753 %
-1.27	-0.211	-36.632 %
0.00	-0.198	-33.277 %
1.27	-0.216	-37.500 %
2.55	-0.277	-56.073 %
3.82		

X-Position	Y-Position	CD reference	CD test
5.356	2.389	0.595	0.397

View Type: Contour Diff
Layer: 3
☐ Tolerance µm 0.010

Figure-5: Image Compare analysis window showing automatically placed measurement slice

4. CONCLUSION

A novel way for the semi-automated analysis of AIMS™ images has been shown. Solutions have been provided to requirements users have dealt with during the progression of the aerial image measurement system from a research tool to a production tool relied upon for most advanced photomasks. Throughput of the analysis process has been improved along with an increase in result stability and reliability due to the reduction in user decisions. The structured process discussed is providing new ways to give users the flexibility to analyze various types of photomask layouts while being confident in the results.

ACKNOWLEGDEMENTS

The authors would like to thanks the Carl Zeiss SMS GmbH software group in Jena, Germany for their dedication and hard work put into this development project.

REFERENCES

1. R. A. Budd, J. Staples, and D. B. Dove, *A New Tool for Phase Shift Mask Evaluation, the Stepper Equivalent Aerial Image Measurement System AIMS*, ***Proc. SPIE*** **2087,** pp. 162-171, 1993.
2. A. Zibold et al, *First results for hyper NA scanner emulation from AIMS 45-193i,* **Proc. SPIE, Vol. 6283**, pp 628312, 2006.
3. Scherübl, T., Dürr, A. C., Böhm, K., et al., *Programmed defects study on masks for 45nm immersion lithography using the novel AIMS 45-193i*, **Proc. of SPIE Vol. 6533**, pg. 653309, 2007.
4. De Bisschop, P., Philipsen, V., Birkner, R., et al., *Using the AIMS 45-193i for hyper-NA imaging applications*, **Proc. of SPIE Vol. 6730**, pg. 67301G, 2007
5. Y. Liu and A. Zakhor, *Binary and phase shifting mask design for optical lithography*, **IEEE Trans. On Semi. Manufacturing (5)**, pp. 138-152, 1992.
6. E. Hendrickx; R. Birkner; M. Kempsell; A. Tritchkov; G. Vandenberghe; T. Scheruebl, *AIMS-45 image validation of contact hole patterns after inverse lithography at NA 1.35*, **Proc. of SPIE Vol. 7122**, 2008.